



Born–Infeld AdS Black Holes as Heat Engines

Clifford V. Johnson

*Department of Physics and Astronomy
University of Southern California
Los Angeles, CA 90089-0484, U.S.A.*

johnson1, [at] usc.edu

Abstract

We study the efficiency of heat engines that perform mechanical work *via* the pdV terms present in the First Law in extended gravitational thermodynamics. We use charged black holes as the working substance, for a particular choice of engine cycle. The context is Einstein gravity with negative cosmological constant and a Born–Infeld non–linear electrodynamics sector. We compare the results for these “holographic” heat engines to previous results obtained for Einstein–Maxwell black holes, and for the case where there is a Gauss–Bonnet sector.

1 Introduction

This paper presents a class of corrections to the efficiency of holographic heat engines which have charged black holes as the working substance. The corrections arise as a result of non-linear extension of the electromagnetic sector, the Born–Infeld action. Holographic heat engines were defined in ref. [1]. They are a natural concept in *extended* gravitational thermodynamics, which, in making the cosmological constant (Λ) dynamical in a theory of gravity, supplies¹ a pressure variable $p = -\Lambda/8\pi$ and its conjugate volume V (see refs. [2–13]). One may extract mechanical work *via* the pdV term in the First Law of Thermodynamics, and so it is possible to define a cycle in state space during which there is a net input heat Q_H flow, a net output flow Q_C and a net output work W , such that $Q_H = W + Q_C$. The efficiency is then $\eta = W/Q_H$. Its value is determined by the equation of state of the system and the choice of cycle in state space. The gravitational solution (a black hole, in our case) supplies the equation of state: The temperature T , entropy S , enthalpy H and other quantities can be defined [2, 14–17], and there are relations between them.

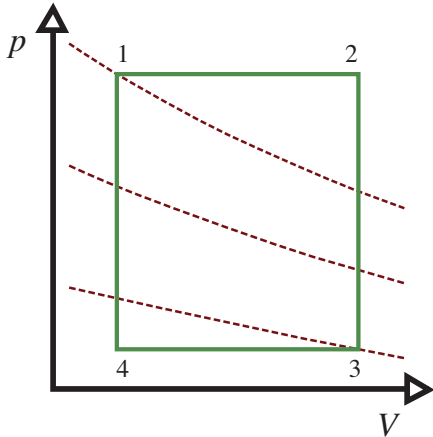


Figure 1: Our engine.

We will choose the cycle given in figure 1, following earlier work in refs. [1, 18], where it is explained why that is a natural choice for static black holes, which we will study here².

The Born–Infeld action [23–25] is a non-linear generalization of the Maxwell action³, controlled by a parameter β :

$$\mathcal{L}(F) = 4\beta^2 \left(1 - \sqrt{1 + \frac{F^{\mu\nu} F_{\mu\nu}}{2\beta^2}} \right), \quad (1)$$

where in the limit $\beta \rightarrow \infty$ we recover the Maxwell action. The completion of Maxwell into Born–Infeld is quite natural in string theory [26], where $1/\beta \propto 2\pi\alpha'$,

i.e. it is like the tension of the string. The corrections about the $\beta \rightarrow \infty$ expansion (the famous zero-slope limit) is an infinite family of α' corrections. In studying the efficiency of our black

¹Here we are using geometrical units where G, c, \hbar, k_B have been set to unity.

²Refs. [19–22] have since done further studies of such heat engines.

³Here, we follow a common strand of terminology in the literature: Strictly speaking, the displayed action (1) is due to Born [23, 24]. In the original $D = 4$ context, the full Born–Infeld action has under the square root a quartic term $(\mathbf{B} \cdot \mathbf{E})^2$ as well as the quadratic term $\mathbf{E}^2 - \mathbf{B}^2$ shown. However, in the case of vanishing magnetic sector (as will be true in this paper), the actions have the same content. The action (1), in any number of dimensions, is often referred to as Born–Infeld in the literature — as is the D -dimensional version of the full action that Born and Infeld wrote [25] (with $\det(\eta_{\mu\nu} + F_{\mu\nu}/\beta)$ under the square root). Thanks to David Chow for prompting the clarification after an earlier version of this manuscript appeared.

hole heat engine as a function of β , we can therefore think of it as capturing the effects of α' -like corrections in some underlying string theory model, but it is not necessary to do so. It is interesting enough to consider the system in its own right.

Another possible context for this study is the fact that we will work in negative cosmological constant (defining a positive pressure), for which such physics has an holographic duality [27–31] to non-gravitational field theories in one dimension fewer, at large N (where N is the rank of a field theory gauge group, or an analogue thereof). As pointed out in ref. [1], since changing Λ involves changing the N (or analogues thereof) of the dual theory, the heat engine cycle is a kind of tour on the *space* of field theories rather than staying within one particular field theory⁴. Our studies therefore concern corrections to the physics of such tours as well, but our focus here will be to study the properties of our new black hole engines in Born–Infeld for their own sake, leaving examination of the implications for those possible applications for another time.

Once we have extracted the efficiency of our engines in the presence of Born–Infeld (and we will do so working in a high temperature limit) we will compare the results to the Einstein–Maxwell case, and also contrast it with the results obtained in ref. [18] for another class of α' -like corrections, the Gauss–Bonnet case. In this way we’ll have studied two distinct classes of corrections to these engines’ efficiency: Corrections to the Einstein sector, and corrections to the Maxwell sector.

2 The Black Holes and the Equation of State

Our Einstein–Hilbert–Born–Infeld bulk action in D -dimensions is:

$$I = \frac{1}{16\pi} \int d^D x \sqrt{-g} (R - 2\Lambda + \mathcal{L}(F)) , \quad (2)$$

with $\mathcal{L}(F)$ given in equation (1). The cosmological constant sets a length scale l according to:

$$\Lambda = -\frac{(D-1)(D-2)}{2l^2} . \quad (3)$$

The black hole has mass and charge parameters m and q , with metric [33–35]

$$ds^2 = -Y(r)dt^2 + \frac{dr^2}{Y(r)} + r^2 d\Omega_{D-2}^2 , \quad (4)$$

where $d\Omega_{D-2}^2$ is the metric on a round $D-2$ sphere with volume ω_{D-2} , and

$$Y(r) = 1 - \frac{m}{r^{D-3}} + \frac{r^2}{l^2} + \frac{4\beta^2 r^2}{(D-1)(D-2)} \left(1 - \sqrt{1 + \frac{(D-2)(D-3)q^2}{2\beta^2 r^{2D-4}}} \right) + \frac{2(D-2)q^2}{(D-1)r^{2D-4}} {}_2F_1 \left[\frac{D-3}{2D-4}, \frac{1}{2}, \frac{3D-7}{2D-4}, -\frac{(D-2)(D-3)q^2}{2\beta^2 r^{2D-4}} \right] , \quad (5)$$

⁴As pointed out in ref. [32] it also involves changing the size of the space the field theories live on.

where ${}_2F_1$ is the hypergeometric function. The gauge potential is:

$$A_t = -\frac{q}{c} \frac{1}{r^{D-3}} {}_2F_1 \left[\frac{D-3}{2D-4}, \frac{1}{2}, \frac{3D-7}{2D-4}, -\frac{(D-2)(D-3)q^2}{2\beta^2 r^{2D-4}} \right], \quad \text{with} \quad c = \sqrt{\frac{2(D-3)}{D-2}}. \quad (6)$$

The mass and charge of the solution are given by:

$$M = \frac{(D-2)\omega_{D-2}}{16\pi} m \quad \text{and} \quad Q = \sqrt{2(D-2)(D-3)} \left(\frac{\omega_{D-2}}{8\pi} \right) q. \quad (7)$$

Given an horizon of radius r_+ (the largest root of $Y(r_+) = 0$), the temperature T , entropy S , and volume V are given by [34–36]:

$$T = \frac{1}{4\pi} \left(16\pi p \frac{r_+}{(D-2)} + \frac{(D-3)}{r_+} + \frac{4\beta^2 r_+^2}{(D-2)} \left(1 - \sqrt{1 + \frac{(D-2)(D-3)q^2}{2\beta^2 r_+^{2D-4}}} \right) \right), \quad (8)$$

$$S = \frac{\omega_{D-2}}{4} r_+^{D-2}, \quad \text{and} \quad V = \frac{\omega_{D-2}}{(D-1)} r_+^{D-1}, \quad (9)$$

where we have used that $p = -\Lambda/8\pi$ and equation (3). The temperature expression (8) can be re-arranged into an equation of state (actually a family of equations of state parameterized by q , which we will keep fixed) in the p – r_+ plane, or equivalently the p – V plane. As noted in ref. [18], in the high temperature limit, the leading behaviour of this equation of state is:

$$pV^{1/(D-1)} \sim T, \quad (10)$$

a sort of ideal gas limit for our black holes. At lower temperatures there can be quite non-trivial behaviour as a coming from multivaluedness of the state curve (generalizing what was found for Reissner–Nordström black holes in refs. [37–39]) giving rise to non-trivial phase transitions [40–43], which will not be our focus here.

3 The Engine Efficiency

3.1 The Specific Heat

The specific heat at constant pressure $C_p \equiv T\partial S/\partial T|_p$ is the next quantity we need. It is most easy to compute it in terms of r_+ , as discussed in ref. [18], and the result is, for general D :

$$C_p = \frac{(D-2)\omega_{D-2}}{4} r_+^{D-2} \times \left(\frac{\frac{16\pi}{(D-2)(D-3)} p r_+^{2D-4} + r_+^{2D-6} + \frac{4\beta^2}{(D-2)(D-3)} \left(1 - \mathcal{R}^{\frac{1}{2}} \right) r_+^{2D-4}}{\frac{16\pi}{(D-2)(D-3)} p r_+^{2D-4} - r_+^{2D-6} + \frac{4\beta^2}{(D-2)(D-3)} \left(1 - \mathcal{R}^{\frac{1}{2}} \right) r_+^{2D-4} + 2(D-2)q^2 \mathcal{R}^{-\frac{1}{2}}} \right), \quad (11)$$

where

$$\mathcal{R} \equiv 1 + \frac{(D-2)(D-3)q^2}{2\beta^2 r_+^{2D-4}}. \quad (12)$$

3.2 The Efficiency η

For our engine cycle defined in figure 1, we have

$$W = (V_2 - V_1) (p_1 - p_4) , \quad (13)$$

where the subscripts refer to the quantities evaluated at the corners labeled (1,2,3,4). The heat flows take place along the top and bottom, with the upper isobar giving the net inflow of heat:

$$Q_H = \int_{T_1}^{T_2} C_p(p_1, T) dT , \quad (14)$$

The efficiency is then $\eta = W/Q_H$.

3.3 The High Temperature Limit

To get an explicit expression for C_p in terms of T so that we can integrate along the isobar, we take a high temperature limit, solving for r_+ perturbatively in a large T expansion, using equation (8), and substituting into (11). We expand V in the same way. For example, in $D = 4$:

$$\begin{aligned} r_+ &= \frac{1}{2} \frac{T}{p} - \frac{1}{4\pi T} + \frac{1}{8} \frac{p(8\pi p q^2 - 1)}{\pi^2 T^3} + \frac{1}{8} \frac{p^2 (16 q^2 p \pi - 1)}{\pi^3 T^5} \\ &\quad + \left(-\frac{1}{32} \frac{p^3 (5 - 120 q^2 p \pi + 192 q^4 p^2 \pi^2)}{\pi^4} - 4 \frac{p^6 q^4}{\pi \beta^2} \right) \frac{1}{T^7} + \dots , \\ V &= \frac{4\pi}{3} r_+^3 = \frac{\pi}{6p^3} T^3 - \frac{1}{4} \frac{T}{p^2} + \frac{q^2}{T} + \frac{1}{48} \frac{(48 q^2 p \pi - 1)}{\pi^2 T^3} \\ &\quad - \frac{1}{32} \frac{p (1 - 48 q^2 p \pi + 128 q^4 p^2 \pi^2 + 128 p^3 q^4 \pi^3 / \beta^2)}{\pi^3 T^5} + \dots , \\ \int C_p dT &= \frac{\pi}{6p^2} T^3 + \frac{1}{8} \frac{(16\pi p q^2 - 1)}{\pi T} + \frac{1}{12} \frac{p (24 q^2 p \pi - 1)}{\pi^2 T^3} \\ &\quad - \frac{1}{5} \left(\frac{3}{32} \frac{p^2 (5 - 160 q^2 p \pi + 320 q^4 p^2 \pi^2)}{\pi^3} + 24 \frac{p^5 q^4}{\beta^2} \right) \frac{1}{T^5} + \dots \quad (15) \end{aligned}$$

and in $D = 5$:

$$\begin{aligned} r_+ &= \frac{3}{4} \frac{T}{p} - \frac{1}{2\pi T} - \frac{p}{3\pi^2 T^3} + \frac{4}{81} \frac{p^2 (32 q^2 \pi^2 p^2 - 9)}{\pi^3 T^5} \\ &\quad + \frac{4}{81} \frac{p^3 (128 q^2 p^2 \pi^2 - 15)}{\pi^4 T^7} + \frac{112}{729} \frac{p^4 (128 q^2 p^2 \pi^2 - 9)}{\pi^5 T^9} \\ &\quad + \left(-\frac{32}{19683} \frac{p^5 (-34560 q^2 p^2 \pi^2 + 10240 q^4 p^4 \pi^4 + 1701)}{\pi^6} - \frac{131072}{19683} \frac{p^{10} q^4}{\pi \beta^2} \right) \frac{1}{T^{11}} + \dots , \end{aligned} \quad (16)$$

with

$$\begin{aligned}
V &= \frac{\pi^2}{2} r_+^4 = \frac{81}{512} \frac{\pi^2}{p^4} T^4 - \frac{27}{64} \frac{\pi T^2}{p^3} + \frac{9}{64 p^2} + \frac{4}{3} \frac{\pi p q^2}{T^2} \\
&\quad + \frac{1}{96} \frac{(256 q^2 p^2 \pi^2 - 3)}{\pi^2 T^4} + \frac{1}{108} \frac{p (640 q^2 p^2 \pi^2 - 9)}{\pi^3 T^6} \\
&\quad - \frac{1}{2916} \frac{p^2 (-40320 \pi^2 p^2 q^2 + 28672 \pi^4 p^4 q^4 + 567 + 16384 q^4 p^5 \pi^5 / \beta^2)}{\pi^4 T^8} + \dots, \\
\int C_p dT &= \frac{81}{512} \frac{\pi^2}{p^3} T^4 - \frac{27}{128} \frac{\pi T^2}{p^2} + \frac{1}{96} \frac{(192 \pi^2 p^2 q^2 - 9)}{\pi T^2} \\
&\quad + \frac{5}{288} \frac{p (256 q^2 p^2 \pi^2 - 9)}{\pi^2 T^4} + \frac{7}{216} \frac{p^2 (320 q^2 p^2 \pi^2 - 9)}{\pi^3 T^6} \\
&\quad - \frac{1}{324} \frac{p^3 (-8064 \pi^2 p^2 q^2 + 4096 \pi^4 p^4 q^4 + 189 + 2048 q^4 p^5 \pi^5 / \beta^2)}{\pi^4 T^8} + \dots
\end{aligned} \tag{17}$$

These expressions for V and $\int C_p dT$ can now be used to compute the efficiency *via* equations (13) and (14), taking their ratio. Both quantities are evaluated at the pressure of the upper isobar, p_1 , and because pV and $\int C_p dT$ have identical leading terms, we have $\eta = (1 - p_4/p_1) + \dots$ with corrections that can be evaluated readily by substitution (see refs. [1, 18] for further discussion).

A striking feature of these expansions is how late β enters: It is at order T^{-5} for $D = 4$ and at order T^{-8} for $D = 5$. This will mean (as we shall see in the next section) that the variation in the efficiency as a function of β will be somewhat understated as compared to the variation with α (the coefficient of the Gauss–Bonnet action) in the companion study of ref. [18]. There, α appears immediately at the next-to-leading term at order T^2 .

4 Two Studies of $\eta(\beta)$

Equipped with our high temperature expansion, we can now study the efficiency as a function of β , seeing how $\eta(\beta)$ behaves as we move away the $\beta = \infty$ (Maxwell) limit. The efficiency in the Einstein–Maxwell limit will be denoted $\eta_0 = \lim_{\beta \rightarrow \infty} \eta(\beta)$. We will study the two schemes that were defined in ref. [18], determined by what parameters of the cycle we specify and hold fixed as we change β .

4.1 Scheme 1

Here, for our engine cycle (see figure 1) we specify the two operating pressures (p_1, p_4) and the two temperatures (T_1, T_2). We can evaluate the efficiency in this scheme as a function of β , seeing how it moves away from the benchmark η_0 of Maxwell electrodynamics.

Actually, at a given value of β we can compare to an important additional benchmark, the Carnot efficiency $\eta_C = 1 - T_C/T_H$, where T_C and T_H are, respectively, the lowest and highest

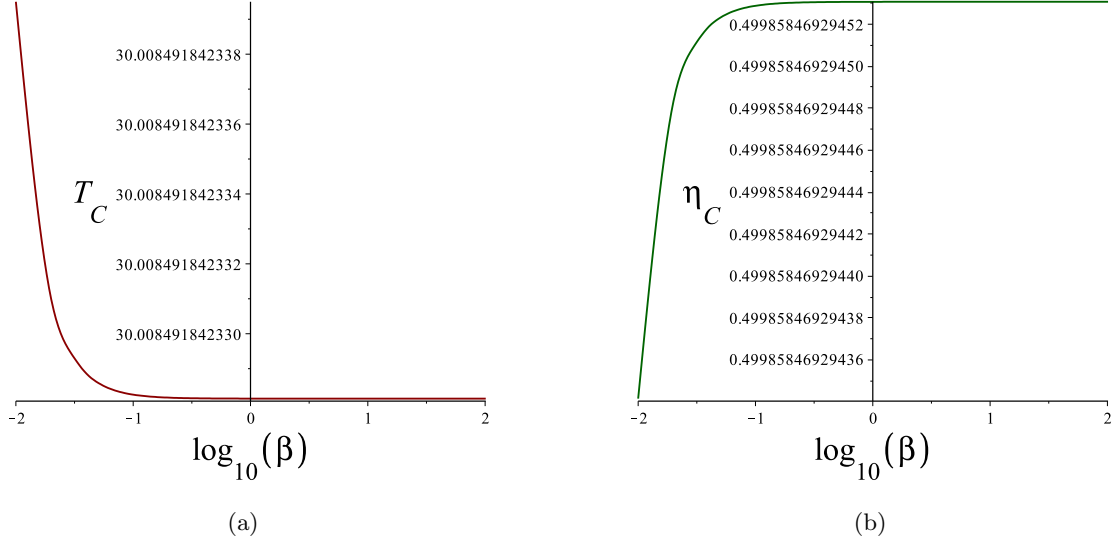


Figure 2: (a) The exact temperature T_C vs. $\log_{10}(\beta)$, in scheme 1. (b) The exact Carnot efficiency η_C , vs. $\log_{10}(\beta)$, also in scheme 1. These quantities were computed using the exact equation of state. See text. (Here, we’ve chosen the values $p_1 = 5, p_4 = 3, T_1 = 50, T_2 = 60$, and $q = 0.1$. The same key features were observed for a range of sample values, including even higher temperatures.)

temperatures our engine can attain. This is the efficiency obtained with a reversible heat engine operating between those two temperatures. Although we’ve specified $T_H \equiv T_2$, η_C changes with β since T_C does: The equation of state must be used to determine $T_4 \equiv T_C$. We observe that as β runs from ∞ toward smaller values T_C increases slowly. Correspondingly, the Carnot efficiency decreases. See figure 2 for the exact T_C and η_C for a sample range $10^{-2} < \beta < 10^2$. The Maxwell limit is to the right. (This is analogous to what was seen in scheme 1 in ref. [18].) As already remarked at the end of the last section, the dependence on β is relatively weak, and for all quantities plotted in this section, the variation is small over this wide range, with most of the change beginning late in the range at a “turnaround region” where, roughly, $\beta \sim 10^{-1}$. All plots are against $\log_{10}(\beta)$ to better display the features.

Figure 3(a) displays the ratio η/η_C and figure 3(b) shows that the ratio η/η_0 , both plotted against $\log_{10}(\beta)$. The Maxwell limit is to the right. In 3(a), it can be seen that the ratio grows slowly for a while and then rises more rapidly in the turnaround region. In 3(b) there is a very slow initial decline before the faster fall in the turnaround region. It is worth comparing this behaviour to that seen in the Gauss–Bonnet case for scheme 1, as exhibited in ref. [18]. We’ll discuss the comparison further in section 5.

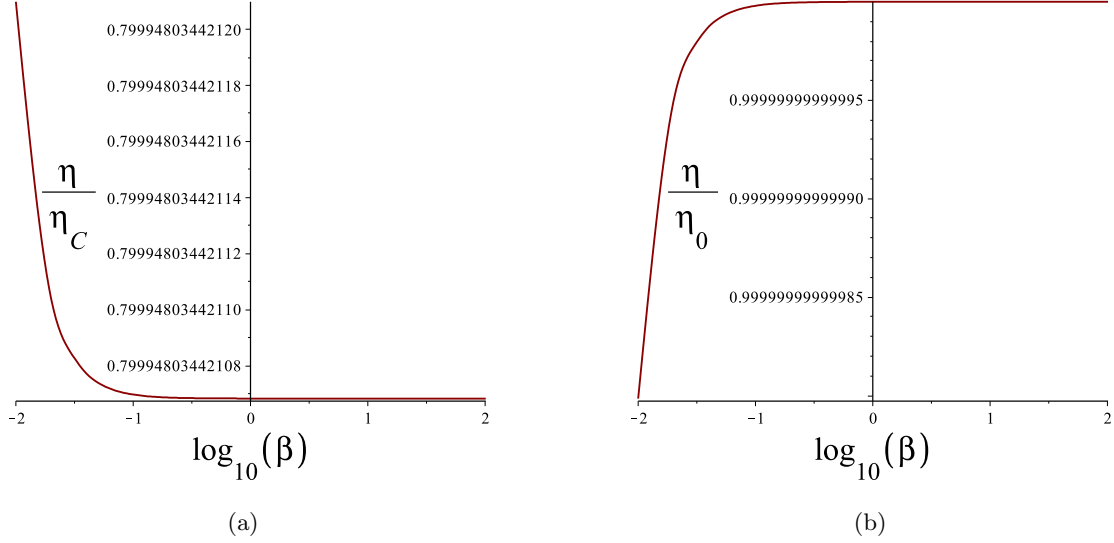


Figure 3: (a) The engine efficiency η/η_C vs. $\log_{10}(\beta)$, in scheme 1. (b) The ratio η/η_0 vs. $\log_{10}(\beta)$ over the same range, also in scheme 1. (See the caption of figure 2 for the parameter values chosen.)

4.2 Scheme 2

In this scheme for our engine (again see figure 1) we instead specify the temperatures (T_2, T_4) , equivalent to specifying (T_H, T_C) , as well as the volumes (V_2, V_4) (which also gives the pair (V_3, V_1)). Now the Carnot efficiency η_C is fixed for all β . Instead, however, the pressures $p_1 = p_2$ and $p_4 = p_3$ must be determined using the equation of state, and so are now β -dependent. (We checked that the pressures in the engine remained physical over the range of $10^{-2} < \beta < 10^2$, which is to be expected since we have fixed our highest and lowest temperatures to be far enough into the high temperature regime.) In figure 4, we again plot the ratios η/η_C and η/η_0 , against $\log_{10}(\beta)$. Again, the Maxwell limit is to the right. We'll discuss these results further in section 5.

It is worth noting that the $D = 4$ case was explored explicitly as well, for each scheme, and the qualitative structure of the results was found to be the same as for the $D = 5$ case explored here, so no detailed results are reported from that case. The features (a slow change followed by the characteristic elbow or knee in the turnaround region) are a bit more pronounced since β appears at slightly higher order: $O(T^{-5})$. It is expected that higher D will also work similarly.

5 Closing Remarks

In ref. [18], the corrections to the geometrical sector, from a Gauss-Bonnet term with coefficient α , were studied for their effect on the efficiency of a heat engine in the same schemes 1 and 2 studied here. In the present study we looked instead at corrections to the Maxwell sector, controlled by

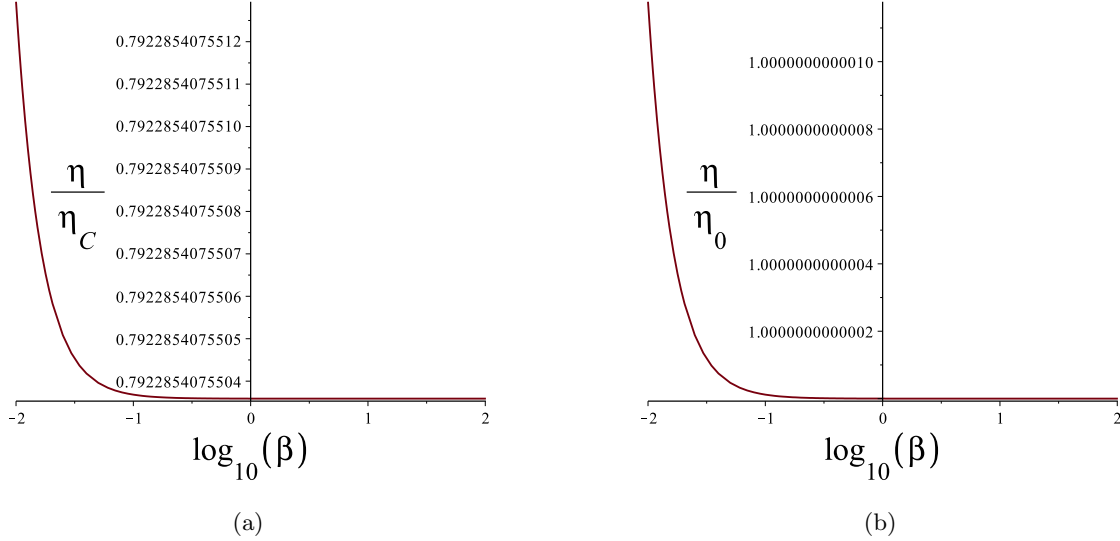


Figure 4: (a) The engine efficiency η/η_C *vs.* $\log_{10}(\beta)$, in scheme 2. (b) The ratio η/η_0 *vs.* $\log_{10}(\beta)$ over the same range, also in scheme 2. (For these examples, $T_2 \equiv T_H = 60$, $V_2 = 33000$, $T_4 \equiv T_C = 30$, $V_4 = 15500$. The same key features were observed for a range of sample values, including even higher temperatures.)

parameter β in the Born–Infeld action, examining their effects on the heat engine efficiency. These two studies reveal features that are in sharp contrast to each other.

The most striking contrast is how weak the β -corrections are compared to the α -corrections, as noted at the end of section 3.3, and as can be seen in all the figures in section 4. The resulting magnitude of the variation in the efficiency with β is of order 10^{-12} . Even after restrictions to the relatively narrow physical window allowed for α , the variations there are many orders of magnitude greater [18]. (Our examples used in each case have the same values for the fixed parameters to allow this comparison.)

There is a much larger window of available values of β to explore, while α is tightly constrained by certain physical requirements. This difference may ultimately be traceable to the fact that α controls just one finite set of correction terms in the action, while in contrast β can explore a much richer range of effects starting with an infinite family of terms (in the sense of expanding the action (1) around the $\beta \rightarrow \infty$ limit) all the way to the effects at small β that generate the turnaround region seen in section 4.

The large (but not infinite) β regime is where we can best compare directly to the small α regime that is the physical window in ref. [18]. Here again, we see some contrasts. In scheme 1, the ratios η/η_C and η/η_0 were seen to increase as the α -corrections were turned on. The opposite is seen here for the ratio η/η_0 . In scheme 2, the behaviour of the ratios are of opposite character for the β variations *vs.* the α , variations, increasing for the former case, and decreasing for the latter.

Acknowledgements

CVJ would like to thank the US Department of Energy for support under grant DE-FG03-84ER-40168, and Amelia for her support and patience.

References

- [1] C. V. Johnson, “Holographic Heat Engines,” *Class. Quant. Grav.* **31** (2014) 205002, [arXiv:1404.5982 \[hep-th\]](#).
- [2] D. Kastor, S. Ray, and J. Traschen, “Enthalpy and the Mechanics of AdS Black Holes,” *Class.Quant.Grav.* **26** (2009) 195011, [arXiv:0904.2765 \[hep-th\]](#).
- [3] M. M. Caldarelli, G. Cognola, and D. Klemm, “Thermodynamics of Kerr-Newman-AdS black holes and conformal field theories,” *Class.Quant.Grav.* **17** (2000) 399–420, [arXiv:hep-th/9908022 \[hep-th\]](#).
- [4] S. Wang, S.-Q. Wu, F. Xie, and L. Dan, “The First laws of thermodynamics of the (2+1)-dimensional BTZ black holes and Kerr-de Sitter spacetimes,” *Chin.Phys.Lett.* **23** (2006) 1096–1098, [arXiv:hep-th/0601147 \[hep-th\]](#).
- [5] Y. Sekiwa, “Thermodynamics of de Sitter black holes: Thermal cosmological constant,” *Phys.Rev.* **D73** (2006) 084009, [arXiv:hep-th/0602269 \[hep-th\]](#).
- [6] E. A. Larranaga Rubio, “Stringy Generalization of the First Law of Thermodynamics for Rotating BTZ Black Hole with a Cosmological Constant as State Parameter,” [arXiv:0711.0012 \[gr-qc\]](#).
- [7] B. P. Dolan, “The cosmological constant and the black hole equation of state,” *Class.Quant.Grav.* **28** (2011) 125020, [arXiv:1008.5023 \[gr-qc\]](#).
- [8] M. Cvetič, G. Gibbons, D. Kubiznak, and C. Pope, “Black Hole Enthalpy and an Entropy Inequality for the Thermodynamic Volume,” *Phys.Rev.* **D84** (2011) 024037, [arXiv:1012.2888 \[hep-th\]](#).
- [9] B. P. Dolan, “Compressibility of rotating black holes,” *Phys.Rev.* **D84** (2011) 127503, [arXiv:1109.0198 \[gr-qc\]](#).
- [10] B. P. Dolan, “Pressure and volume in the first law of black hole thermodynamics,” *Class.Quant.Grav.* **28** (2011) 235017, [arXiv:1106.6260 \[gr-qc\]](#).

- [11] M. Henneaux and C. Teitelboim, “The Cosmological Constant as a Canonical Variable,” *Phys.Lett.* **B143** (1984) 415–420.
- [12] C. Teitelboim, “The Cosmological Constant as a Thermodynamic Black Hole Parameter,” *Phys.Lett.* **B158** (1985) 293–297.
- [13] M. Henneaux and C. Teitelboim, “The Cosmological Constant and General Covariance,” *Phys.Lett.* **B222** (1989) 195–199.
- [14] J. D. Bekenstein, “Black holes and entropy,” *Phys.Rev.* **D7** (1973) 2333–2346.
- [15] J. D. Bekenstein, “Generalized second law of thermodynamics in black hole physics,” *Phys.Rev.* **D9** (1974) 3292–3300.
- [16] S. Hawking, “Particle Creation by Black Holes,” *Commun.Math.Phys.* **43** (1975) 199–220.
- [17] S. Hawking, “Black Holes and Thermodynamics,” *Phys.Rev.* **D13** (1976) 191–197.
- [18] C. V. Johnson, “Gauss-Bonnet Black Holes and Holographic Heat Engines Beyond Large N,” [arXiv:1511.08782 \[hep-th\]](#).
- [19] A. Belhaj, M. Chabab, H. El Moumni, K. Masmar, M. B. Sedra, and A. Segui, “On Heat Properties of AdS Black Holes in Higher Dimensions,” *JHEP* **05** (2015) 149, [arXiv:1503.07308 \[hep-th\]](#).
- [20] J. Sadeghi and K. Jafarzade, “Heat Engine of black holes,” [arXiv:1504.07744 \[hep-th\]](#).
- [21] E. Caceres, P. H. Nguyen, and J. F. Pedraza, “Holographic entanglement entropy and the extended phase structure of STU black holes,” *JHEP* **09** (2015) 184, [arXiv:1507.06069 \[hep-th\]](#).
- [22] M. R. Setare and H. Adami, “Polytropic black hole as a heat engine,” *Gen. Rel. Grav.* **47** (2015) no. 11, 133.
- [23] M. Born, “Modified Field Equations with a Finite Radius of the Electron,” *Nature* **132** (1933) 282–282.
- [24] M. Born, “Quantum theory of the electromagnetic field,” *Proc. Roy. Soc. Lond.* **A143** (1934) 410–437.
- [25] M. Born and L. Infeld, “Foundations of the new field theory,” *Proc. Roy. Soc. Lond.* **A144** (1934) 425–451.

- [26] G. W. Gibbons, “Aspects of Born-Infeld theory and string / M theory,” *Rev. Mex. Fis.* **49S1** (2003) 19–29, [arXiv:hep-th/0106059](#) [[hep-th](#)]. [[324\(2001\)](#)].
- [27] J. M. Maldacena, “The large n limit of superconformal field theories and supergravity,” *Adv. Theor. Math. Phys.* **2** (1998) 231–252, [hep-th/9711200](#).
- [28] E. Witten, “Anti-de sitter space and holography,” *Adv. Theor. Math. Phys.* **2** (1998) 253–291, [hep-th/9802150](#).
- [29] S. S. Gubser, I. R. Klebanov, and A. M. Polyakov, “Gauge theory correlators from non-critical string theory,” *Phys. Lett.* **B428** (1998) 105–114, [hep-th/9802109](#).
- [30] E. Witten, “Anti-de sitter space, thermal phase transition, and confinement in gauge theories,” *Adv. Theor. Math. Phys.* **2** (1998) 505–532, [hep-th/9803131](#).
- [31] O. Aharony, S. S. Gubser, J. M. Maldacena, H. Ooguri, and Y. Oz, “Large n field theories, string theory and gravity,” *Phys. Rept.* **323** (2000) 183–386, [hep-th/9905111](#).
- [32] A. Karch and B. Robinson, “Holographic Black Hole Chemistry,” [arXiv:1510.02472](#) [[hep-th](#)].
- [33] S. Fernando and D. Krug, “Charged black hole solutions in Einstein-Born-Infeld gravity with a cosmological constant,” *Gen. Rel. Grav.* **35** (2003) 129–137, [arXiv:hep-th/0306120](#) [[hep-th](#)].
- [34] R.-G. Cai, D.-W. Pang, and A. Wang, “Born-Infeld black holes in (A)dS spaces,” *Phys. Rev.* **D70** (2004) 124034, [arXiv:hep-th/0410158](#) [[hep-th](#)].
- [35] T. K. Dey, “Born-Infeld black holes in the presence of a cosmological constant,” *Phys. Lett.* **B595** (2004) 484–490, [arXiv:hep-th/0406169](#) [[hep-th](#)].
- [36] D.-C. Zou, S.-J. Zhang, and B. Wang, “Critical behavior of Born-Infeld AdS black holes in the extended phase space thermodynamics,” *Phys. Rev.* **D89** (2014) no. 4, 044002, [arXiv:1311.7299](#) [[hep-th](#)].
- [37] A. Chamblin, R. Emparan, C. V. Johnson, and R. C. Myers, “Charged AdS black holes and catastrophic holography,” *Phys. Rev.* **D60** (1999) 064018, [hep-th/9902170](#).
- [38] A. Chamblin, R. Emparan, C. V. Johnson, and R. C. Myers, “Holography, thermodynamics and fluctuations of charged ads black holes,” *Phys. Rev.* **D60** (1999) 104026, [hep-th/9904197](#).

- [39] D. Kubiznak and R. B. Mann, “P-V criticality of charged AdS black holes,” *JHEP* **1207** (2012) 033, [arXiv:1205.0559 \[hep-th\]](#).
- [40] S. Fernando, “Thermodynamics of Born-Infeld-anti-de Sitter black holes in the grand canonical ensemble,” *Phys. Rev.* **D74** (2006) 104032, [arXiv:hep-th/0608040 \[hep-th\]](#).
- [41] Y. S. Myung, Y.-W. Kim, and Y.-J. Park, “Thermodynamics and phase transitions in the Born-Infeld-anti-de Sitter black holes,” *Phys. Rev.* **D78** (2008) 084002, [arXiv:0805.0187 \[gr-qc\]](#).
- [42] S. Gunasekaran, R. B. Mann, and D. Kubiznak, “Extended phase space thermodynamics for charged and rotating black holes and Born-Infeld vacuum polarization,” *JHEP* **1211** (2012) 110, [arXiv:1208.6251 \[hep-th\]](#).
- [43] R. Banerjee and D. Roychowdhury, “Critical behavior of Born Infeld AdS black holes in higher dimensions,” *Phys. Rev.* **D85** (2012) 104043, [arXiv:1203.0118 \[gr-qc\]](#).